

# Shear-Wave Velocity of Surficial Geologic Sediments in Northern California: Statistical Distributions and Depth Dependence

Thomas L. Holzer,<sup>a)</sup> M.EERI, Michael J. Bennett,<sup>a)</sup> Thomas E. Noce,<sup>a)</sup> and John C. Tinsley, III<sup>a)</sup>

Shear-wave velocities of shallow surficial geologic units were measured at 210 sites in a 140-km<sup>2</sup> area in the greater Oakland, California, area near the margin of San Francisco Bay. Differences between average values of shear-wave velocity for each geologic unit computed by alternative approaches were in general smaller than the observed variability. Averages estimated by arithmetic mean, geometric mean, and slowness differed by 1 to 8%, while coefficients of variation ranged from 14 to 25%. With the exception of the younger Bay mud that underlies San Francisco Bay, velocities of the geologic units are approximately constant with depth. This suggests that shear-wave velocities measured at different depths in these surficial geologic units do not need to be normalized to account for overburden stress in order to compute average values. The depth dependence of the velocity of the younger Bay mud most likely is caused by consolidation. Velocities of each geologic unit are consistent with a normal statistical distribution. Average values increase with geologic age, as has been previously reported. Velocities below the water table are about 7% less than those above it.

[DOI: 10.1193/1.1852561]

## INTRODUCTION

Values and vertical gradients of shear-wave velocity ( $V_S$ ) are important physical properties of soils. They are used in both basic and applied geophysics and civil engineering. An important application of  $V_S$  is to predict amplification of ground shaking at soil sites. This amplification is commonly referred to as site response. Shear-wave velocity is used both to classify the amplification potential of soil sites and to calibrate models for site-specific predictions. The significance of amplification of seismic waves by shallow soils has been demonstrated in many earthquakes, but it was particularly significant in the 1985 Michoacan, Mexico, and 1989 Loma Prieta, California, earthquakes, where it was the major cause of damage (Anderson et al. 1986, Holzer 1994). Many building codes now require consideration of site response when estimating the seismic demand on a structure and rely on a time-averaged  $V_S$  to a depth of 30 m ( $V_{S30}$ ) for this evaluation (see Borchardt 2002; ICBO 1997). In addition, several investigations have recently used correlations between geologic units and  $V_S$  in conjunction with surficial geo-

<sup>a)</sup> U.S. Geological Survey, MS 977, 345 Middlefield Rd., Menlo Park, CA 94025

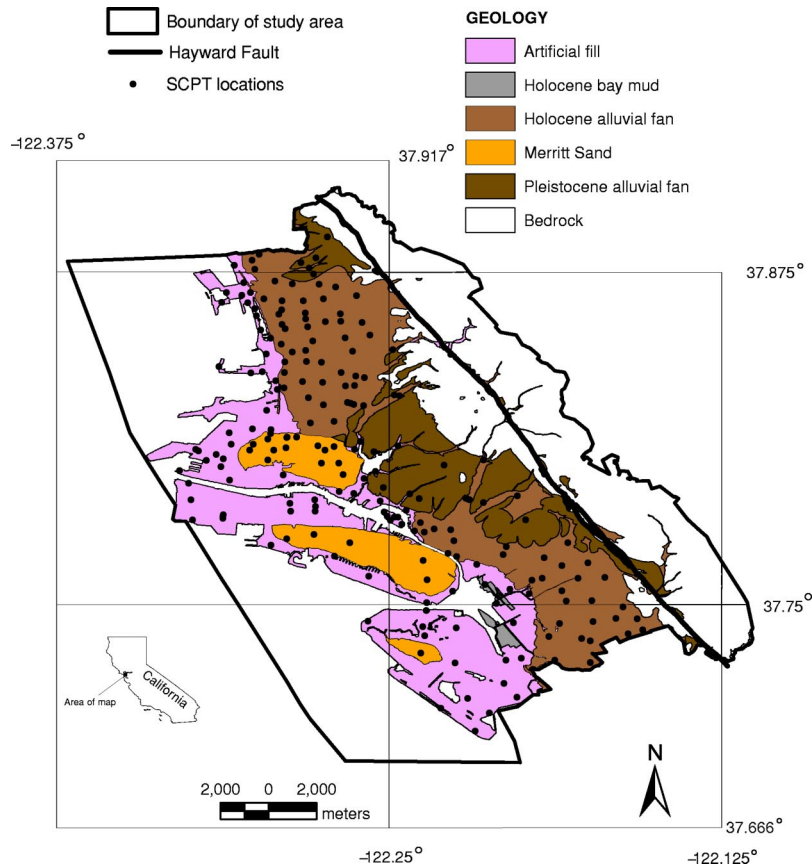


**Figure 1.** Simplified surficial geologic map of study area with SCPT locations. Geology is modified from Helley and Graymer (1997).

logic maps to portray  $V_{S30}$  geographically (Holzer et al. 2002, Wills et al. 2000). Understanding the  $V_S$  properties of geologic units is important for future refinements of microzonation maps of site amplification based on surficial geologic maps.

The purpose of this article is to describe the spatial and statistical distributions of  $V_S$  of shallow Holocene and Pleistocene geologic sediments from 210 seismic cone penetration tests (SCPT) that were conducted in a 140-km<sup>2</sup> area near the eastern margin of San Francisco Bay, California (Figure 1). The area lies within the communities of Alameda, Berkeley, Emeryville, and Oakland. These data were collected to improve mapping of National Earthquake Hazards Reduction Program (NEHRP) site classes in the study area (Holzer et al. 2002). The implications of alternative velocity assignments for the NEHRP map are evaluated by Holzer et al. (2005). Correlations of  $V_S$  with SCPT penetration resistance and geologic age are described by Piratheepan (2002). The purpose here is take advantage of the large number of measurements of  $V_S$  to analyze the depth dependence and statistical properties of  $V_S$ . The results indicate that (1) the  $V_S$

**Table 1.** Unified Soil Classification (USC) and approximate age of geologic units

Geologic Unit	USC Classification	Geologic age (years)
Artificial fill	SM	Modern
Younger Bay mud	CL	Holocene (<8,000)
Holocene alluvial fan	CL, SM	Holocene (<15,000)
Merritt sand	SM	Pleistocene (80,000–10,000)
Pleistocene alluvial fan	CL, SM	Pleistocene (>116,000)

of shallow geologic deposits is approximately constant with depth, (2) the  $V_S$  of geologic units is consistent with a normal statistical distribution, and (3) natural variability is more significant than how average velocities are computed. These data are also a significant addition to the more than 700 geographically dispersed profiles of  $V_S$  in the United States that are currently available (Wills and Silva 1998).

### STUDY AREA AND GEOLOGIC SETTING

The study area extends from the city of Berkeley, California, southward to the city of Oakland, along the coastal plain adjacent to San Francisco Bay. The surficial geology is shown in Figure 1. The area contains five major surficial geologic units in addition to bedrock—artificial fill, younger San Francisco Bay mud, Holocene alluvial fan, Merritt sand, and Pleistocene alluvial fan. Soil classifications and approximate geologic ages of the surficial geologic units are shown in Table 1. The study area can be subdivided into three broad regions from a surficial geology perspective. The dominant surficial unit in the western region is artificial fill that rests on Holocene deposits that consist primarily of younger Bay mud. Most of the artificial fill consists of sands that were hydraulically emplaced. The fill in general is not compacted except for a thin surface layer. The surficial units in the central region, which is east of the filled area, are alluvial fan deposits. The youngest fan deposit is Holocene in age and was part of an active alluvial fan until it was stabilized by urbanization. The Holocene alluvial fan deposits unconformably overlie alluvial fan deposits of Pleistocene age, which crop out in the eastern part of the central region. In the eastern region, bedrock, ranging from consolidated Cretaceous sediments to Jurassic volcanic rocks, crops out (Graymer 2000). Locally within the western and central regions, the Holocene deposits rest on Merritt sand, which is primarily a windblown sand that was deposited when sea level was lower during the Wisconsin glaciation and exposed the bottom of San Francisco Bay to subaerial conditions. Thicknesses of the Holocene deposits are variable, and locally may exceed 30 m. The thickness of the artificial fill averages about 3 m, but locally exceeds 10 m. Ground water is generally encountered at less than 3 m in most of the study area.

Examples of the shallow subsurface geology are shown in the SCPT profiles in Figure 2. The profiles include tip and friction ratio and the  $V_S$  of each geologic unit. The geologic units are based on the surficial geologic units mapped by Helley and Graymer (1997). The uppermost geologic unit in each sounding was determined from the surficial

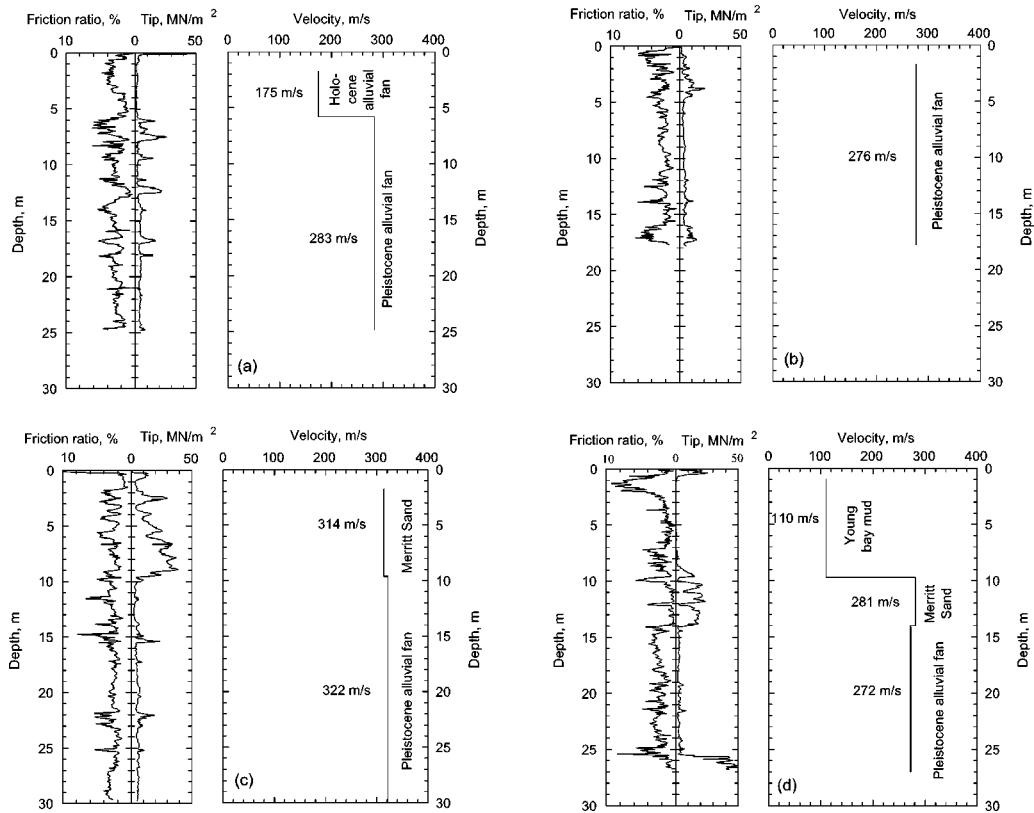


**Figure 2.** Selected sounding profiles of CPT friction ratio and tip resistance with  $V_S$  of geologic units: (a) OAK099, Holocene alluvial fan overlying Pleistocene alluvial fan; (b) OAK070, Pleistocene alluvial fan; (c) OAK007, Merritt sand overlying Pleistocene alluvial fan; and (d) OAK041, artificial fill, younger Bay mud, Merritt sand, and Pleistocene alluvial fan.

geologic map. In most instances, each geologic unit had a distinctive SCPT signature and range of  $V_S$ . Thus, by simultaneously conducting cone penetration tests and  $V_S$  measurements, the major geologic units penetrated by a sounding usually could be identified. For soundings in which unit identification was ambiguous, sampling and comparison with adjacent soundings were used. The SCPT data used for this investigation are available on the Internet at <http://quake.usgs.gov/prepare/cpt/>.

The sounding in Figure 2a was conducted in the central region, and penetrated Holocene and Pleistocene alluvial fan deposits. The sounding in Figure 2b was conducted in the eastern part of the central region, and penetrated only Pleistocene alluvial fan. The sounding in Figure 2c penetrated Pleistocene Merritt sand and underlying Pleistocene alluvial fan. The sounding in Figure 2d was conducted in the western region and penetrated artificial fill, younger Bay mud, Pleistocene Merritt sand, and Pleistocene alluvial fan.

## METHODOLOGY

$V_S$  data in this investigation were obtained by SCPT using the downhole method (see Lunne et al. 1997). A 23-ton truck was used to push a 3.6-cm-diameter instrumented cone with a seismometer into the soil. The average penetration depth was 18 m, and the deepest penetration was 51 m. This method is applicable only to soil sites; it cannot be used to measure  $V_S$  at bedrock sites. The seismometer, which sits 0.25 m above the tip of the cone, is a horizontally oriented, single-component, velocity transducer. Horizontally polarized shear waves are generated at the land surface by striking on a vertical face of a steel box with a sledgehammer. The travel time for the vertically propagating shear wave is the time between the hammer blow and the arrival of the shear wave at the seismometer. Travel times typically were measured in the present study at 2-m-depth intervals. Because the strike plate is offset 0.96 m on the ground from where the SCPT penetrates the ground surface, the observed shear wave does not propagate to the seismometer on a truly vertical path; computation of  $V_S$  requires a correction to take the added travel distance caused by this offset into account. The correction was made here to the measured travel time by computing a pseudo-travel time from the measured travel time using a simple cosine correction (Eidsmoen et al. 1985). This allows use of the inverse of the slope of the pseudo-travel time versus depth to compute  $V_S$ .

The horizontal offset used to make the correction was the distance between the closest edge of the strike plate and the penetration point of the SCPT. Some practitioners use the distance between the middle of the plate and the penetration point of the SCPT (see Campanella et al. 1986). The edge of the plate was used because the beginning of shear-wave pulse recorded by the seismometer presumably is generated by the closest part of the steel plate. Fortunately, the choice of the part of the plate from which to measure the horizontal offset only affects the estimate of  $V_S$  in the upper few meters because the offset used here was small (Butcher and Powell 1995).

Shear-wave velocities of geologic units in each sounding were computed with two approaches. In the first approach, the  $V_S$  of each entire geologic unit penetrated in a given sounding was calculated. In the second approach, the  $V_S$  of each 2-m-depth interval in a sounding was computed and assigned to the appropriate geologic unit.

The first approach is illustrated in Figure 3. By this approach, the  $V_S$  of each geologic unit in a sounding was estimated by manually fitting a line to the pseudo-travel time versus depth data within the unit. The inverse of the slope of the line is the  $V_S$ . The slope was determined manually instead of with an ordinary least-squares approach because geologic units commonly were not very thick. This thinness did not permit a robust regression analysis to estimate unit velocity because travel times were measured only every 2 m. Thus, a unit that was only 4 m thick would have only two travel-time measurements in most cases. In fact, velocities were commonly estimated with only three depth/travel time pairs because units were often less than 6 m thick. A secondary consideration that prompted the manual line fitting was the effect of thin (<2-m-thick) layers of sand within units. The higher  $V_S$  of these coarse-grained layers causes small perturbations in travel time plots. Because these layers are conspicuous in the cone penetration test profile, their impact on  $V_S$  can be minimized by manually fitting the data.

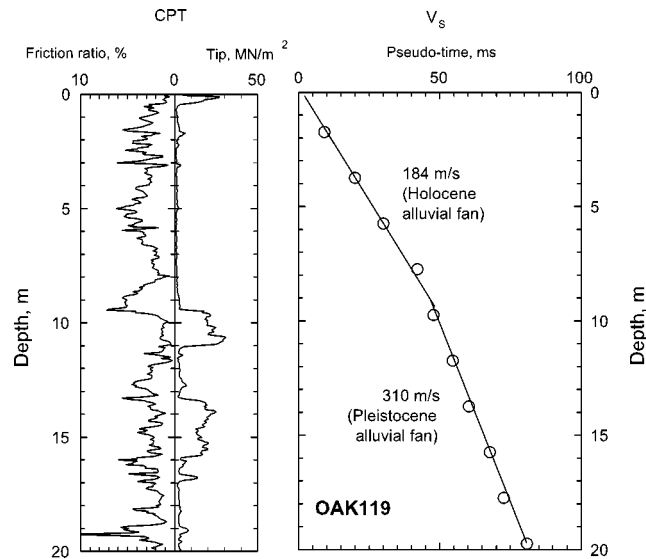


**Figure 3.** SCPT sounding profile with pseudo-travel times.

The second approach consisted of computing  $V_S$  values for each 2-m-depth interval by differencing the pseudo-travel times measured 2 m apart in a specific sounding. The  $V_S$  for each interval was assigned to the appropriate geologic unit, and the midpoint of the interval was used as the depth value for the measurement. Velocities for intervals that straddled the contact between geologic units were excluded from the compilation.

It should be noted that the  $V_S$  reported here for the younger Bay mud is for the upper or soft member of the mud (Trask and Rolston 1951, Treasher 1963), which is the predominant component of the younger Bay mud in the study area. The younger Bay mud contains a stiff lower member that has been informally referred to as the semi-consolidated member (Treasher 1963). The  $V_S$  of the stiff member is higher than that of the rest of the unit and is readily recognized in SCPT soundings by its higher tip resistance. It is not geographically continuous in the study area and was observed in only a few soundings. In addition to the stiff lower member, the younger Bay mud in the study area frequently includes a thin (<2 m) basal sand of reworked Merritt sand that was deposited during the time of the Holocene marine transgression. The primary impact of including these other components of the younger Bay mud would be to increase the unit average and standard deviation of  $V_S$ , respectively, by about 10 and 40%. General conclusions are not affected.

## DATA

Average  $V_S$  values from both approaches are compared in Table 2. Three different average velocities were computed—an arithmetic mean, a geometric mean, and an average based on slowness, which is the inverse of velocity (see Brown et al. 2002 for a discussion). Because the number of measurements of 2-m-interval  $V_S$  in each geologic

**Table 2.** Comparison of average  $V_S$  computed with 3 approaches for each geologic unit

$V_S$ (m/s)	Fill (0–1.75 m)	Fill (>1.75 m)	Younger Bay mud	Holocene alluvial fan	Pleistocene alluvial fan	Merritt sand
<i>2-m interval <math>V_S</math></i>						
Arithmetic Mean	184	159	128	224	330	325
Geometric Mean	177	156	126	219	321	319
(Average Slowness) <sup>-1</sup>	170	152	118	214	312	311
<i>Entire geologic unit <math>V_S</math></i>						
Arithmetic Mean	184	163	109	209	319	332
Geometric Mean	177	158	108	207	316	328
(Average Slowness) <sup>-1</sup>	170	153	106	204	313	324

unit decreases with depth, the averages shown for the 2-m intervals in Table 2 are the means of the averages computed at each depth. So, for example, if 20, 15, and 10 measurements of  $V_S$ , respectively, were available at depths of 2, 4, and 6 m in a given unit, averages were first computed for each depth and then the mean of these averages was reported as the unit average in Table 2. If all 2-m-interval  $V_S$  measurements had been averaged together, the large number of shallow measurements would have dominated unit averages. To compute the average 2-m-interval  $V_S$  of each unit based on slowness, values of slowness were computed for each 2-m interval within each unit. The mean slowness values at each depth in a unit were then averaged to produce an average slowness for the unit. The average velocity based on slowness, which is reported in Table 2, is the inverse of the average slowness.

The statistics—arithmetic mean, standard deviation, and sample size—of  $V_S$  are shown in Table 3. The variability of  $V_S$  for entire geologic units is illustrated in Figure 4 with the histograms of  $V_S$ ; the variability of the 2-m-interval  $V_S$  is indicated by the scatter in Figure 5. The standard deviation of the 2-m-interval  $V_S$  was computed in a similar

**Table 3.** Statistics of  $V_S$  distributions—mean, standard deviation, and sample size—of geologic units

Statistical Properties	Fill (0–1.75 m)	Fill (>1.75 m)	Younger Bay mud	Holocene alluvial fan	Pleistocene alluvial fan	Merritt sand
<i>2-m interval</i>						
Arithmetic Mean (m/s)	184	159	128	224	330	325
Standard Deviation (m/s)	52	36	26	51	84	66
Sample size	68	58	135	166	659	178
<i>Entire geologic unit</i>						
Arithmetic Mean (m/s)	184	163	109	209	319	332
Standard Deviation (m/s)	52	46	19	38	44	52
Sample size	68	36	69	89	111	57

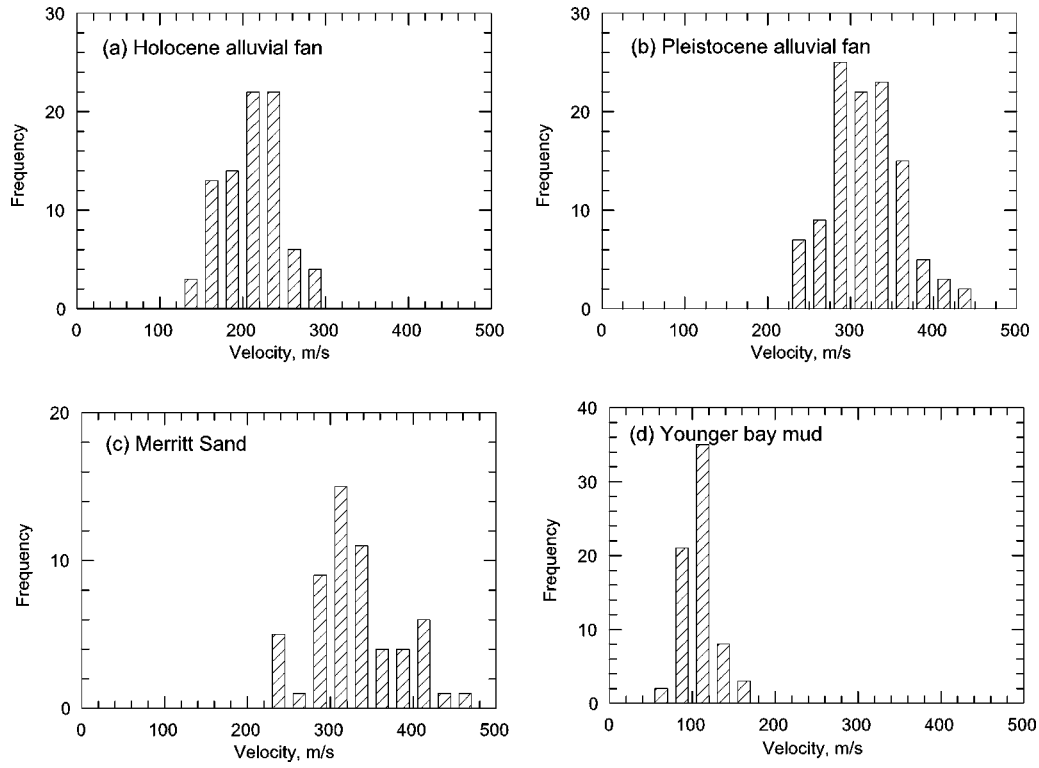


**Figure 4.** Histograms of  $V_S$  of entire geologic units.

manner to that used to compute the means. Values of standard deviation were computed for each depth and then these values were averaged to produce the means reported in Table 3.

The standard deviation of the 2-m-interval  $V_S$  reported in Table 3, herein referred to as the observed standard deviation, results from a combination of measurement error and real formational (or material) variability. Because the square of the observed standard deviation is the sum of the squares of the standard deviations attributable to measurement error and formational variability, the formational variability can be computed if the other two variabilities are known.

The primary cause of measurement error is the accuracy of timing the arrival of the shear wave. Because signal processing improved over the course of the field investigation, picking the arrival time became more accurate. To estimate the standard deviation of the timing error, several records were picked repeatedly and the standard deviation of the time picks ( $s_t$ ) was computed. Early records yielded an  $s_t$  of 0.7 ms, while later records yielded an  $s_t$  of 0.2 ms. To estimate the uncertainty in  $V_S$  caused by the inaccuracy in picking the arrival time, the standard deviation of the time picks ( $s_t$ ) was added to the average 2-m travel time for each geologic unit and then a new 2-m-interval velocity was computed. The difference between these velocities is approximately the stan-

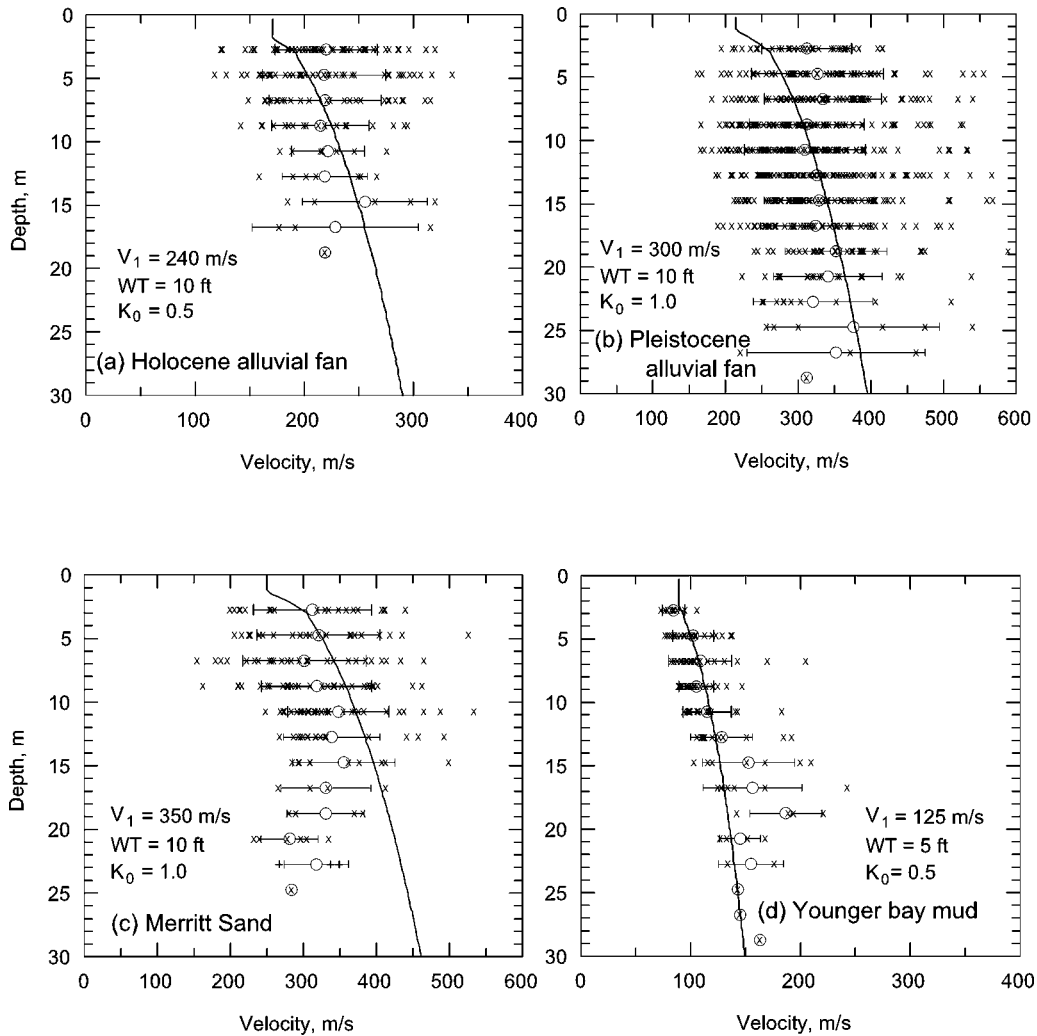


**Figure 5.** Two-meter-interval  $V_S$  versus depth of (a) Holocene alluvial fan, (b) Pleistocene alluvial fan, (c) Merritt sand, and (d) younger Bay mud. Mean and one standard deviation, respectively, are indicated by circle and horizontal line with brackets. Curves show depth dependency predicted by Equation 1 with the parameters shown on the graph. Note  $V_S$  scale varies between panels.

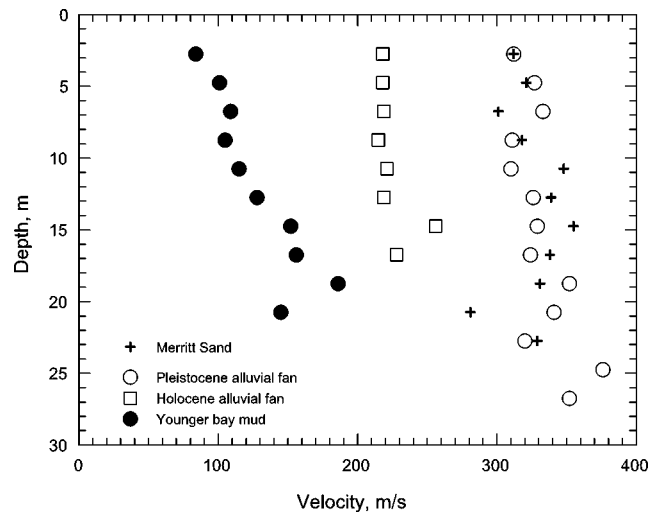
dard deviation of the velocity measurement error. The estimated velocity measurement error and resulting formational standard deviation are shown in Table 4. Estimates of formational standard deviations for both the original (0.7 ms) and improved (0.2 ms) signal processing are shown in Table 4. Although formational variability cannot be inferred precisely from Table 4 because measurement error progressively decreased during

**Table 4.** Estimated formational variability of 2-m-interval  $V_S$  of geologic units

Standard deviation of 2-m $V_S$ (m/s)	Younger Bay mud	Holocene alluvial fan	Pleistocene alluvial fan	Merritt sand
Observed $s_t=0.7$ ms	27	52	76	66
Measurement	5	20	46	46
Formational	27	48	61	48
$s_t=0.2$ ms				
Measurement	1	6	13	13
Formational	27	52	75	65

the course of the field investigation, Table 4 indicates that formational variability is a significant component of the observed variability, even under the less accurate picking condition ( $s_t=0.7$  ms).

Figure 5 also shows the variation of  $V_S$  of each geologic unit with respect to depth. The artificial fill is not included because it is less than 4.5 m thick in most of the study area. Despite the scatter,  $V_S$  appears to be approximately constant with depth for the Merritt sand and Holocene and Pleistocene alluvial fans. Only the  $V_S$  of the younger Bay mud markedly increases with depth (Figure 5a). These trends are even clearer when only mean values of the 2-m-interval  $V_S$  are plotted (Figure 6). Linear regression of the 2-m-interval  $V_S$  for younger Bay mud with respect to depth ( $z$ ) yields  $V_S=3.99z+75.2$ ; the least-squares fit for slowness ( $V_S^{-1}$ ) is  $V_S^{-1}=-0.000288z+0.0120$ . Both regressions included the uncertainty of  $V_S$  (or  $V_S^{-1}$ ) at each depth as in-

**Figure 6.** Mean values of 2-m-interval  $V_S$  versus depth for each geologic unit.

licated by the standard deviation of the 2-m-interval  $V_S$  (or  $V_S^{-1}$ ) (see Press et al. 1992, pp. 655–656). The least-squares fit was performed only on the upper 21 m of the younger Bay mud because of the small number of  $V_S$  measurements at each depth below 21 m (see Figure 5d).

The data described here also confirm Hamilton's (1976) conclusion, based on laboratory measurements, that the position of the water table has only a modest influence on  $V_S$ . As was noted by Hardin and Richart (1963), moisture decreases the shear modulus of granular material. The effect of the water table on  $V_S$  was evaluated by comparing measurements above the water table in 23 soundings with measurements below the water table in 30 soundings. Comparisons were restricted to the Holocene alluvial fan and comparisons are for measurements made at comparable depths, mostly at 2.75 m. Water tables were measured directly in the open hole created by each sounding. The average  $V_S$  measured above the water table was 7% higher than it was below the water table.

## DISCUSSION

Differences between average values of  $V_S$  for each geologic unit computed by alternative approaches are small (Table 2). Averages differ by as little as 6 to 7% for the Merritt sand and Holocene and Pleistocene alluvial fans to as much as 17% for the younger Bay mud. Despite the small differences, the intended application of the average  $V_S$  may dictate a specific approach. For example, computing averages with slowness emphasizes the lowest velocity values. For evaluations of site response, averages based on slowness are more appropriate for computing  $V_{S30}$ . The inverse of the slowness values for both the 2-m intervals and entire unit consistently produced the lowest  $V_S$  values. Comparison of entire unit averages with 2-m-interval mean values for geologic units was not consistent. Entire unit averages compared to 2-m-interval mean values were lower for the younger Bay mud and Holocene alluvial fan and higher for the Merritt sand.

Uncertainty introduced by observed variability is more important than the approach used to compute the average  $V_S$ . The variability of  $V_S$  within geologic units is much larger than the differences introduced by using the different methods to compute the average  $V_S$ . Coefficients of variation—the ratio of standard deviation to the mean—range from about 16% for the entire geologic unit to about 22% for the 2-m-interval  $V_S$ .

A major contributor to variability of each geologic unit is the range of depositional environments represented by the sediment that are included within each geologic unit. For example, the Merritt sand, although consisting primarily of windblown deposits, includes fluvial deposits laid down between dunes; the Holocene and Pleistocene alluvial fan deposits include levee, channel, and flood-basin facies (Helley and Graymer 1997). These environments cause deposition of a variety of soil textures that can influence  $V_S$ .

Previous compilers of  $V_S$  have proposed that the distribution of  $V_S$  of geologic units is lognormal (EPRI 1993). The distributions of  $V_S$  of the geologic units investigated here, however, are consistent with a normal distribution. This is suggested by the histograms of  $V_S$  of the entire geologic unit (Figure 4) and the near equality of the arithmetic and geometric means (Table 2). This may be in part the result of the small coefficients of variation of the geologic units considered here. When the coefficient of variation is less than 25%, normal and lognormal distributions are difficult to distinguish. A formal test

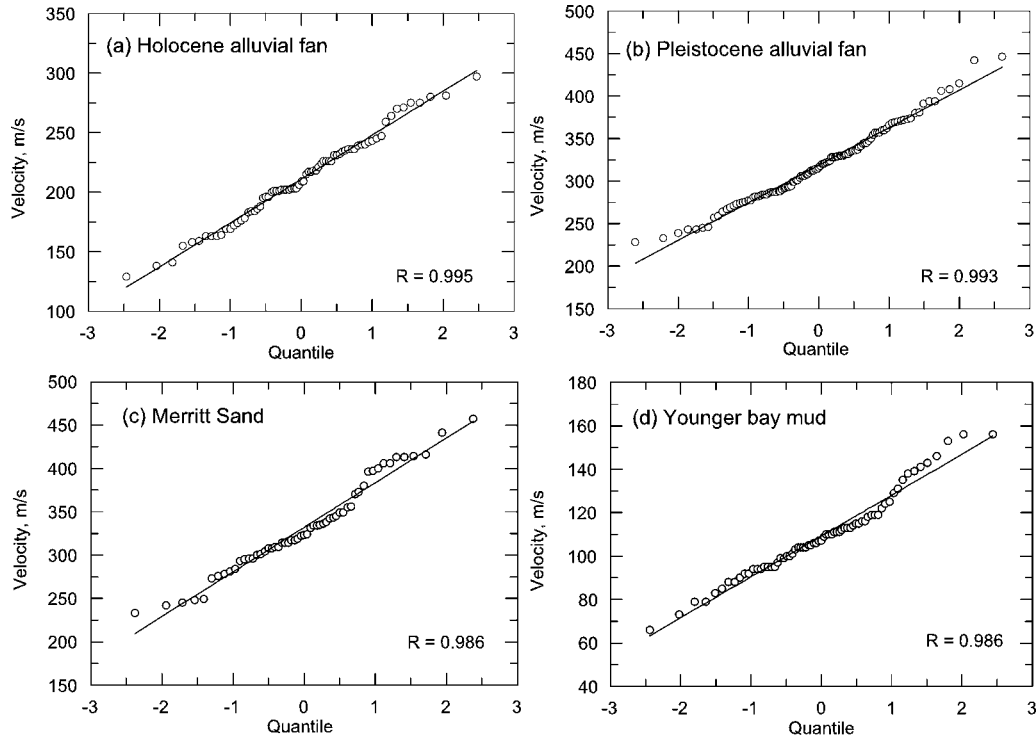


**Figure 7.** Normal quantile plots of  $V_S$  for each geologic unit. Normally distributed data plot on a straight line. A linear regression trend line and its correlation coefficient are also shown for each unit.

of normality is presented in Figure 7, which shows normal quantiles plots of  $V_S$  for each geologic unit (Devore and Farnum 1999). Normally distributed  $V_S$  values plot as a straight line in this format. Correlation coefficients for each plot indicate the correlations are consistent with normality (see Shapiro and Wilk 1965).

The absence of a significant vertical gradient of  $V_S$  in the Merritt sand and Holocene and Pleistocene alluvial fans is relevant to the determination of average unit velocities when  $V_S$  is measured at multiple depths. In the situation here, the primary purpose for collecting the  $V_S$  data was to build a shallow regional three-dimensional velocity model and compute time-averaged velocities to a 30-m depth based on average velocities of geologic units. Because  $V_S$  was measured at different depths, we were concerned that an average of the measured values might be misleading because of the potential effect of overburden stress on  $V_S$ . Accordingly we considered normalizing the field  $V_S$  values for overburden stress before averaging. In fact, the purpose of Figure 5 was to develop the empirical relationship for the normalization. However, the approximately constant velocity with depth in Figure 5 for each geologic unit indicates that such normalization is unnecessary.

Normalization of  $V_S$  to a reference overburden stress is based primarily on laboratory tests of the dependence of  $V_S$  of homogeneous soils on confining pressure (e.g., Hardin and Drnevich 1972, Krizek et al. 1974). It is most commonly used in geotechnical studies of liquefaction that are based on measurements of  $V_S$ . Typically, field  $V_S$  measurements in sands are normalized to a reference effective overburden stress in order to compare measurements obtained at different depths (e.g., Andrus and Stokoe 2000). Following the procedure for correcting standard and cone penetration testing, several investigators have proposed that field values of  $V_S$  be normalized to a reference overburden stress. Robertson et al. (1995) proposed the following normalization:

$$V_{S1} = V_S \left( \frac{P_A}{\sigma'_V} \right)^{0.25} \left( \frac{1}{K_0} \right)^{0.125} \quad (1)$$

where  $V_{S1}$  is the normalized  $V_S$ ;  $P_A$  is the reference pressure (usually 100 kPa);  $\sigma'_V$  is the effective overburden stress; and  $K_0$  is the coefficient of lateral stress at rest, i.e., the ratio of horizontal to vertical effective stress under natural conditions.

The solid lines in Figure 5 show the predicted depth dependence of  $V_S$  based on Equation 1 for each geologic unit if it is assumed that a unit has a constant  $V_{S1}$ . The predicted field velocity profiles are based on assumed parameters shown on each graph.  $K_0$  was assumed equal to 0.5 and 1.0, respectively, for the Holocene and Pleistocene deposits; average depths to ground water were used. With the exception of the younger Bay mud, observed mean values are not in general agreement with the predicted profile.

The cause of the absence of a significant vertical gradient of  $V_S$  that is consistent with Equation 1 is beyond the scope of this investigation. However, the observations here are in situ, whereas Equation 1 is based primarily on laboratory observation. Sediments investigated here have had time to undergo diagenesis. In fact, weathering of materials in spot samples was a criterion used to recognize Pleistocene sediment. We speculate that diagenesis may affect the soil structure and reduce the apparent sensitivity of the shear modulus to increasing pressure. In general, the tip and friction ratio of individual soundings in fine-grained sediment other than the younger Bay mud also did not show a depth dependency, which is consistent with the absence of a depth dependency of  $V_S$  in these soundings. This can be seen in the CPT profiles in Figure 2.

Upon first inspection, the depth profiles of  $V_S$  presented here also are inconsistent with depth profiles of  $V_S$  presented by Wills and Silva (1998). In their profiles,  $V_S$  increases markedly with depth. The apparent inconsistency is an artifact of how the profiles in each investigation were compiled. The profiles presented here only include 2-m-interval velocities for specific geologic units. The profiles presented by Wills and Silva (1998) include velocities of units underlying the surficial unit. Although their profiles are identified by surficial unit, each profile includes measurements in older, and presumably faster, geologic units beneath the surficial unit. Their surficial-unit designation only indicates the unit that the boring initially penetrated at the ground surface.

The depth dependence of  $V_S$  of the younger Bay mud most likely is caused by consolidation rather than directly by stress effects. Hamilton (1976) previously proposed such a mechanism to explain depth dependence of  $V_S$  in fine-grained marine sediment.

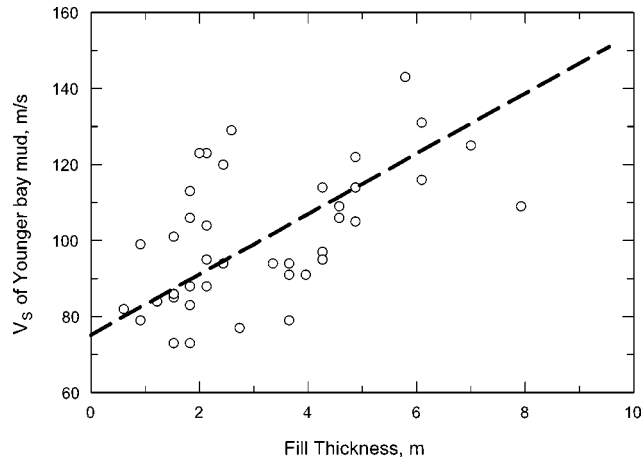


**Figure 8.**  $V_S$  at the top of younger Bay mud versus thickness of overlying artificial fill. Dashed line is relation predicted by the observed linear regression of  $V_S$  versus depth in the younger Bay mud as modified to take the higher density of the fill into account.

The evidence for consolidation is shown in Figure 8. The velocity data in Figure 8 are the 2-m-interval  $V_S$  values for the younger Bay mud measured immediately beneath the artificial fill. Each value is plotted against the thickness of the overlying fill. Note that in general  $V_S$  increases with the thickness of fill. The trend of the data in Figure 8 can be predicted with the linear regression of  $V_S$  for the younger Bay mud,  $3.99z + 75.2$ , if the observed gradient, 3.99 m/s per m, is multiplied by the ratio of the buoyant unit weights of the fill and younger Bay mud. Using a ratio of 1.99 yields the dashed line in Figure 8. The ratio is based on buoyant unit weights of 68 and 34 lbs/ft<sup>3</sup>, respectively, for the fill and soft member of the younger Bay mud (see Lee and Praszker 1969, p. 56; Goldman 1969, p. 22). If consolidation of the mud from the load imposed by the artificial fill, most of which was emplaced about 60 years ago, is assumed to be essentially complete (see Lee and Praszker 1969, p. 72), the agreement of the predicted trend with the data plotted in Figure 8 implies that the depth dependence of  $V_S$  of the younger Bay mud is caused by consolidation. The observation of the higher  $V_S$  beneath the fills also explains the higher  $V_{S30}$  values reported by Wills and Silva (1998) in areas where relatively thick artificial fill rests on younger Bay mud.

An increase of  $V_S$  with geologic age is also observed in Figure 6, an observation that has been reported in many previous investigations (e.g., Fumal 1978). Holocene deposits represented by Holocene alluvial fan and Bay mud sediment are slower than Pleistocene deposits represented by Merritt sand and Pleistocene alluvial fan deposits. The younger Bay mud, a soft estuarine mud, which has remained submerged, is easily the slowest soil in the study area. Deposition of the younger Bay mud commenced when rising sea level, caused by melting of glacial ice during the waning of the last ice age, began to refill San Francisco Bay. Sea level reached the study area 6,000 to 8,000 years ago (Atwater et al. 1977). Because deposition of younger Bay mud has continued to the present, the age of

the mud decreases progressively upward from about 8,000 years old at its base. Deposition of the Holocene alluvial fan deposits was triggered in response to latest Pleistocene climate changes that occurred between 10,000 and 15,000 years ago; the precise age of the basal Holocene in the study area is not known. Deposition has continued to the present, and the Holocene alluvial fan deposits interfinger with younger Bay mud in the subsurface. The slightly greater  $V_S$  of the Holocene alluvial fan relative to younger Bay mud is attributable to the combined effects of its coarser texture and its history of subaerial deposition and exposure. The Pleistocene alluvial fan deposits and Merritt sand have the highest  $V_S$  in the study area. The Merritt sand was deposited during the last glacial epochs, approximately 10,000 to 80,000 years ago. The Pleistocene fans probably were active surfaces of deposition mainly during the sea-level high stands of the last major interglacial epoch (Marine Isotope Substage 5e) from about 132,000 to 116,000 years ago (Shackleton et al. 2002).

Although the primary objective here was to determine the  $V_S$  of geologic units to permit the use of geologic maps for seismic microzonation, correlations of  $V_S$  with SCPT penetration resistance and geologic age were also evaluated in a separate study (Piratheepan 2002). In general, the  $V_S$  of Pleistocene sediment in the study area was found to be 20 to 50% higher than the  $V_S$  of Holocene sediment with similar cone resistances.

## CONCLUSIONS

The purpose of this article was to describe the statistical and spatial distributions of  $V_S$  of shallow Holocene and Pleistocene geologic sediments in a 140-km<sup>2</sup> area near the eastern margin of San Francisco Bay, California. Differences between average values of  $V_S$  for each geologic unit computed by alternative methods—arithmetic mean, geometric mean, and slowness—are small. Averages for entire units differ by as little as 1 to 3%. Averages for 2-m-interval  $V_S$  differ from 2 to 8%. The observed variability of  $V_S$  within a specific geologic unit in general is greater than the variability introduced by the method that is used to compute the average  $V_S$ . Coefficients of variation range from about 16% for the entire geologic unit to about 22% for the 2-m-interval  $V_S$ . Values of  $V_S$  measured in each geologic unit are consistent with a normal statistical distribution. The  $V_S$  of each geologic unit, with the exception of the younger Bay mud, is approximately constant with depth. Field  $V_S$  measurements did not need to be normalized for overburden stress in order to compute average  $V_S$  values of geologic units. The depth dependence of the younger Bay mud appears to be caused by consolidation in response to the weight of the overburden. Velocities below the water table are about 7% less than those above it.

## ACKNOWLEDGMENTS

Reviews and constructive comments by USGS reviewers David M. Boore and Ronald D. Andrus and the *Earthquake Spectra* reviewers, who included Stephen Dickenson, are greatly appreciated. Jon B. P. Fletcher helped with the statistical analyses. Amy C. Padovani prepared Figure 1. The SCPT truck was purchased under the PG&E-USGS CRADA.

## REFERENCES

- Anderson, J. G., Bodin, P., Brune, J. N., Prince, J., Singh, S. K., Quass, R., and Onate, M., 1986. Strong ground motion from the Michoacan, Mexico, earthquake, *Science* **233**, 1043–1049.
- Andrus, R. D., and Stokoe, K. H., II, 2000. Liquefaction resistance of soils from shear-wave velocity, *J. Geotech. Geoenviron. Eng.* **126** (11), 1015–1025.
- Atwater, B. F., Hedel, C. W., and Helley, E. J., 1977. Late Quaternary depositional history, Holocene sea-level changes, and vertical crustal movement, Southern San Francisco Bay, California, *U.S. Geol. Surv. Prof. Paper* 1014.
- Borcherdt, R. D., 2002. Empirical evidence for site coefficients in building code provisions, *Earthquake Spectra* **18** (2), 189–217.
- Brown, L. T., Boore, D. M., and Stokoe, K. H., II, 2002. Comparison of shear-wave slowness profiles at ten strong-motion sites from noninvasive SASW measurements and measurements made in boreholes, *Bull. Seismol. Soc. Am.* **92** (8), 3116–3133.
- Butcher, A. P., and Powell, J. J. M., 1995. The effects of geologic history on the dynamic measurement of the stiffness of soils, *11th European Conference on the Soil Mechanics and Foundation Engineering, Proceedings, Copenhagen*, pp. 27–36.
- Campanella, R. G., Robertson, P. K., and Gillespie, D., 1986. *Seismic Cone Penetration Test, Use of In Situ Tests in Geotechnical Engineering*, 6th edition, ASCE Geotechnical Special Publication, pp. 116–130.
- Devore, J. L., and Farnum, N. R., 1999. *Applied Statistics for Engineers and Scientists*, Duxbury Press, Pacific Grove, CA, 577 pp.
- Eidsmoen, T., Gillespie, D., Lunne, T., and Campanella, R. G., 1985. *Test with UBC Seismic Cone at Three Norwegian Research Sites*, Norwegian Geotechnical Institute 59040-1.
- Electric Power Research Institute (EPRI), 1993. Guidelines for determining design basis ground motions, in *Volume 2: Appendices for Ground Motion Estimation—Appendix 6.A: Probabilistic Model of Soil-Profile Variability*, EPRI TR-102293.
- Fumal, T. E., 1978. Correlation between seismic wave velocities and physical properties of geologic materials, San Francisco Bay region, California, *U.S. Geol. Surv. Open-File Report* 78-1067.
- Goldman, H. B., 1969. Geology of San Francisco Bay, in *Geologic and Engineering Aspects of San Francisco Bay Fill*, edited by H. B. Goldman, California Division of Mines and Geology *Special Report* 97, Sacramento, CA, pp. 11–29.
- Graymer, R. W., 2000. Geologic map and map database of the Oakland Metropolitan Area, Alameda, Contra Costa, and San Francisco Counties, California, *U.S. Geol. Surv. Misc. Field Studies Map* 2342.
- Hamilton, E. L., 1976. Shear-wave velocity versus depth in marine sediments: A review, *Geophysics* **41** (5), 985–996.
- Hardin, B. O., and Drnevich, V. P., 1972. Shear modulus and damping in soils: Measurement and parameter effects, *J. Soil Mech. Found. Div.* **98** (6), 603–624.
- Hardin, B. O., and Richart, F. E., Jr., 1963. Elastic waves in granular soils, *J. Soil Mech. Found. Div.* **89** (1), 33–65.
- Helley, E. J., and Graymer, R. W., 1997. Quaternary geology of Alameda County, and parts of Contra Costa, Santa Clara, San Mateo, San Francisco, Stanislaus, and San Joaquin Counties, California: A digital database, *U.S. Geol. Surv. Open-File Report* 97-97.
- Holzer, T. L., 1994. Loma Prieta damage largely attributed to enhanced ground shaking, *EOS Trans. Am. Geophys. Union* **75** (26), 299–301.

- Holzer, T. L., Bennett, M. J., Noce, T. E., Padovani, A. C., and Tinsley, J. C., III, 2002. Liquefaction hazard and shaking amplification maps of Alameda, Berkeley, Emeryville, Oakland, and Piedmont: A digital database, *U.S. Geol. Surv. Open-File Report 02-296* (<http://geopubs.wr.usgs.gov/open-file/of02-296>).
- Holzer, T. L., Padovani, A. C., Bennett, M. J., Noce, T. E., and Tinsley, J. C., III, 2005. Mapping NEHRP site classes, *Earthquake Spectra*, accepted for publication.
- International Conference of Building Officials (ICBO), 1997. *Uniform Building Code*, Whittier, CA, 1411 pp.
- Krizek, R. J., McLean, F. G., and Giger, M. W., 1974. Effect of particle characteristics on wave velocity, *J. Geotech. Eng.* **100** (1), 89–104.
- Lee, C. H., and Praszker, M., 1969. Bay mud developments and related structural foundations, in *Geologic and Engineering Aspects of San Francisco Bay Fill*, edited by H. B. Goldman, California Division of Mines and Geology *Special Report 97*, Sacramento, CA, pp. 41–85.
- Lunne, T., Robertson, P. K., and Powell, J. J. M., 1997. *Cone Penetration Testing in Geotechnical Practice*, Spon Press, London, 312 pp.
- Piratheepan, P., 2002. Estimating Shear-Wave Velocity from SPT and CPT Data, master's thesis, Clemson University, 184 pp.
- Press, W. H., Teukolsky, S. A., Vetterling, W. T., and Flannery, B. P., 1992. *Numerical Recipes in Fortran: The Art of Scientific Programming*, 2nd edition, Cambridge University Press, Cambridge, 963 pp.
- Robertson, P. K., Sasitharan, S., Cunning, J. C., and Segoo, D. C., 1995. Shear-wave velocity to evaluate in-situ state of Ottawa sand, *J. Geotech. Eng.* **121** (3), 262–303.
- Shackleton, N. J., Chapman, M., Sanchez-Goni, M. F., Pailler, D., and Lancelot, Y., 2002. The classic marine isotope substage 5e, *Quaternary Research* **58** (1), 14–16.
- Shapiro, S. S., and Wilk, M. B., 1965. An analysis of variance test for normality (complete samples), *Biometrika* **52**, 591–611.
- Trask, P. S., and Rolston, J. W., 1951. Engineering geology of San Francisco Bay, California, *Bull. Geol. Soc. Am.* **62** (9), 1079–1110.
- Treasher, R. C., 1963. Geology of the sedimentary deposits in San Francisco Bay, California, in *Short Contributions to California Geology*, California Division of Mines and Geology *Special Report 82*, Sacramento, CA, pp. 11–24.
- Wills, C. J., Petersen, M., Bryant, W. A., Reichle, M., Saucedo, G. J., Tan, S., Taylor, G., and Treiman, J., 2000. A site-conditions map for California based on geology and shear-wave velocity, *Bull. Seismol. Soc. Am.* **90** (6B), S187–S208.
- Wills, C. J., and Silva, W., 1998. Shear-wave velocity characteristics of geologic units in California, *Earthquake Spectra* **14** (3), 533–556.

(Received 7 January 2003; accepted 7 June 2004)